Available online at www.sciencedirect.com
ScienceDirect
Sensors and Actuators B 131 (2008) 279–284
SENSORS AND ACTUATORS B CHEMICAL
www.elsevier.com/locate/snb

High sensitivity photonic crystal biosensor incorporating nanorod structures for enhanced surface area

Wei Zhang, Nikhil Ganesh, Ian D. Block, Brian T. Cunningham *

Nano Sensors Group, Micro and Nanotechnology Laboratory, University of Illinois at Urbana-Champaign, 208 North Wright Street, Urbana, Illinois 61801, United States

Received 7 February 2007; received in revised form 18 October 2007; accepted 12 November 2007
Available online 22 November 2007

Abstract

The surface area of a photonic crystal biosensor is greatly enhanced through the incorporation of a porous TiO_2 film possessing the structure of nanorods into the device. The film is deposited by the glancing angle deposition technique in an e-beam evaporation system. The sensitivity of high surface area sensors is compared with sensors without the high surface area coating. Results for detection of polymer films, large proteins and small molecules indicate up to a four-fold enhancement of detected adsorbed mass density.

Keywords: Biosensor; Surface area; Photonic crystal; Nanostructure; Sensitivity; Glancing angle deposition

1. Introduction

Label-free optical biosensors have emerged as important tools for pharmaceutical research, diagnostic testing, and environmental monitoring [1,2]. Development of sensor designs that enhance sensitivity is especially important because it allows detection of lower concentrations of analytes and detection of small molecules with a higher signal-to-noise ratio. Recently, optical biosensors based on photonic crystals (PCs) have attracted widespread interest due to their ability to concentrate light into extremely small volumes and to obtain very high local electromagnetic field intensities, resulting in reflection/transmission properties that are tuned by the adsorption of chemical and biomolecular materials. These include one and two-dimensional surface PCs (also referred to as guided mode resonance filters) [3–6], three-dimensional opal and inverse opal structures [7,8], PCs with microcavities [9,10], and PC waveguides [11,12].

Because the response of a biosensor generally depends on the interaction of an analyte with a selective immobilized capture ligand on the sensor surface, increasing the surface area of the sensor generally improves the sensitivity through a higher density of the capture ligand. One commercially successful method for increasing ligand surface area has been the use of polymer hydrogels such as dextran [13,14] to extend the surface area for binding into a three-dimensional volume within the evanescent field region of surface plasmon resonance sensors. Other methods involve: (1) porous silicon-based structures by electrochemical etching [15–19], (2) coatings of nanostructured dielectrics by chemical vapor deposition [20,21], microcapillary pipetting [21,22], and sol–gel processes [23], and (3) coatings of high surface area polymers by electrophoretic deposition [21] and spray-on technique [24]. All these methods typically require complex procedures for deposition and/or functionalization using liquid-based processes, or high temperature annealing which is not suitable for plastic-based sensor structures. Therefore, enhancement of biosensor surface area using a simpler technique would be advantageous, especially if it would be a part of the sensor fabrication process, and performed inexpensively and uniformly over large areas.

Glancing angle deposition (GLAD) [25] has been shown to be a method able to create thin films with very high porosities and surface-area-to-volume ratios. By orientating the incoming flux at an oblique angle, the self-shadowing effect during the deposition results in a porous film with a structure composed of isolated vertical nanorods. This technique has been used in various applications such as dielectric reflectors [26], optical filters [27], liquid crystal displays [28], and substrates for surface

* Corresponding author. Tel.: +1 217 265 6291.
E-mail address: bcunning@uiuc.edu (B.T. Cunningham).

0925-4005/$ – see front matter © 2007 Elsevier B.V. All rights reserved.
doi:10.1016/j.snb.2007.11.017

enhanced Raman scattering [29]. In biosensor applications, thin films deposited by GLAD have been used to increase the immobilization density of glucose-oxidase to a surface [30], but to our knowledge, this technique has not been applied to label-free optical biosensors.

In this work, we show the enhancement of PC biosensor sensitivity through application of a thin nanorod coating to the sensor surface by GLAD. We demonstrate up to 4× sensitivity improvement compared to sensors without the nanorod coating. Sensitivity is compared for detecting polymer film adsorption, large protein adsorption and detection of a small molecule. This method may be broadly applied to any type of biosensor—optical, acoustic, or otherwise, to enhance sensitivity.

2. Materials & methods

2.1. Sensor fabrication

Biosensor fabrication begins with a nanoreplica molding process in which a thin layer of liquid UV-curable polymer is squeezed between a flexible polyester sheet, and a silicon "master" wafer that acts as a molding tool, as described in previous research [3]. The silicon wafer is etched with a negative image of the desired surface structure pattern, which in this case is a linear grating with a period of 550 nm and a groove depth of 170 nm, as shown in Fig. 1. After the epoxy is cured, the polyester sheet with the sensor structure is peeled away from the silicon wafer. An 80 nm thin film of TiO_2 is sputtered onto the sensor surface as the last step of sensor fabrication. The biosensors are cut from the polyester sheet and attached with adhesive to form the bottom surface of standard 96-well format microplates [1]. The PC structure described above is designed to support guided mode resonances [31,32] at particular wavelengths. When the structure is illuminated with TM polarized (electric field perpendicular to the grating lines) white light at normal incidence, the reflected spectrum consists of a sharp resonant peak with peak wavelength value (PWV) of 860 nm and full width half maximum of 3 nm when the sensor surface is immersed in water. As protein is deposited onto the sensor surface, the dielectric permittivity of material in contact with the structure changes, resulting in a shift of the PWV to a longer wavelength.

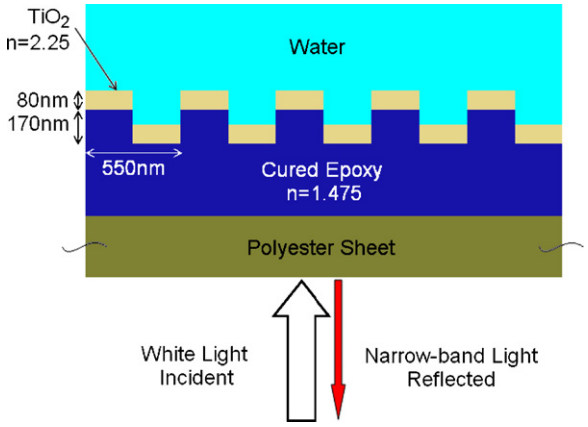

Fig. 1. Cross-section of the PC biosensor structure. The sensor is illuminated at normal incidence with TM polarized white light. The sensor structure reflects back only a narrow band of wavelengths, centered around the peak wavelength value. The reflected spectrum is measured by a spectrometer that determines shifts of PWV due to biochemical binding on the sensor surface.

2.2. Nanorod film deposition

Glancing angle deposition of a TiO_2 layer with nanorod structures onto the sensor surface is performed in an e-beam deposition system (Denton Vacuum) with a base pressure of 2.0×10^{-6} Torr and a deposition rate of 8 Å/s. The sensor is tilted so that the incoming flux of evaporated material is at a glancing angle of $\theta = 3.0^\circ$ from the sensor surface, as shown in Fig. 2a. In order to minimize the shadowing effect between grating lines, the incoming flux must be parallel to the grating sidewalls and no substrate rotation is used during deposition. Also, no substrate heating is used in order to minimize the mobility of the addatoms. Refractive index of the nanorod film that is co-deposited on a silicon wafer positioned next to the sensor is measured by a spectroscopic ellipsometer (Woollam). Nanorod films with a thickness of 85 nm were deposited upon PC biosensors that were previously prepared with a dense layer of TiO_2

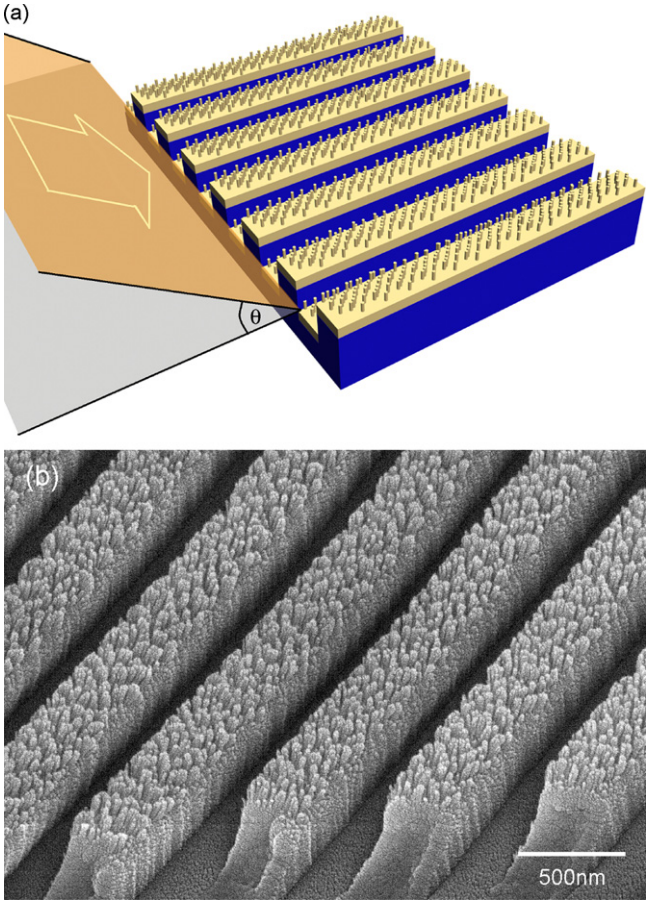

Fig. 2. (a) Schematic of the GLAD setup and (b) SEM photo of the nanorod-coated sensor. The GLAD process utilizes deposition of an 85 nm film of TiO_2 on the surface of an otherwise complete PC biosensor structure. Deposition occurs by orienting the PC grating lines parallel to the direction of evaporated TiO_2 flux, where the flux is incident on the substrate surface at an angle of $\theta = 3.0^\circ$.

applied by sputtering, as described above. Two types of device structures are compared in the current study: sensors with and without an added nanorod coating.

2.3. Assay protocol

To compare biosensor sensitivity between sensors with and without the nanorod coating, a 4-step assay protocol was performed, as shown in the inset of Fig. 4, intended to demonstrate how the available sensor surface area interacts with different types of molecules. The initial step in the protocol is to coat the sensor with a proprietary polymer film that can conform to the available exposed surface area in a single monolayer. The polymer consists of a long, narrow molecular chain with a high density of amine (NH_2) functional groups available along its backbone. The polymer adheres to the TiO_2 sensor surface by noncovalent interaction, and is considered to be small enough to fit between adjacent rods in the nanorod film. Therefore, the biosensor PWV shift measured during attachment of the polymer film should reflect the enhancement of surface area due to the nanorod film. The sensor was immersed in a 0.625% solution of polymer in water for 28 h, followed by washing 3 times with water, followed by a measurement of PWV shift.

The second step of the protocol involves functionalizing the amine groups within the deposited polymer film by exposure to glutaraldehyde (GA; $C_5H_8O_2$; MW = 100 Da). Due to the small molecular weight of GA, it is also expected to penetrate the nanorod surface structure. The GA will form a stable covalent attachment to the polymer amine groups, and therefore measurement of PWV shift due to incorporation of GA is also expected to provide a measurement of available surface area for biomolecular binding. Because the chemical structure of GA allows the molecule to perform as a bifunctional linker, this step enables subsequent covalent attachment of protein molecules with exposed amine moieties. For this step, each well of the sensor was exposed to 60 μl GA solution (25% in water; Sigma–Aldrich) for 4 h, followed by a wash step and a measurement of PWV shift.

The third step of the protocol is to attach a large protein to the sensor surface. Streptavidin (SA; MW = 60,000 Da), was selected for this purpose. As a large, globular protein with reported size of ~8 nm [33,34], SA binding will only be enhanced if it is capable of fitting within the nanorod structure. 60 μl of SA (0.5 mg/ml in water; Prozyme) was added to the sensor and allowed to incubate for 40 h, followed by a wash step and a PWV shift measurement to quantify the amount of SA attachment. At this step, several wells of the sensor were not exposed to SA and later they would be used as reference wells to subtract the nonspecific binding signal of the biotin binding step.

The final step of the protocol is to expose a small molecule, biotin (MW = 244 Da), to the immobilized SA. Each SA contains four possible biotin binding sites, with a very high affinity bond (dissociation constant $K_d = 10^{-15}$ M [35]). This step is intended to demonstrate the proper functionality of the SA protein immobilized within the nanorod film, and the ability of small molecules to penetrate the structure after it is loaded with protein. Due to the discrepancy in molecular weight between SA and biotin, the expected biosensor PWV shift is smaller by the relation:

$$\Delta\mathrm{PWV}_{\mathrm{Biotin}}(\mathrm{expected}) = \frac{4 \times \mathrm{MW}_{\mathrm{Biotin}}}{\mathrm{MW}_{\mathrm{SA}}} \times \Delta\mathrm{PWV}_{\mathrm{SA}}(\mathrm{measured}) \quad (1)$$

Ten microliter of biotin (1 mg/ml in water; Sigma–Aldrich) was added to the sensor surface with 200 μl of water buffer and the kinetics of the binding signal was continuously monitored. The above 4-step protocol was carried out in parallel on sensors with and without the added nanorod film.

3. Results

The self-shadowing effect of the GLAD results in the formation of nanorod structures uniformly coated on the sensor surface, as shown in the SEM photo of Fig. 2b. The refractive index of the nanorod film is measured to be $n = 1.45$ at a wavelength of 860 nm, while TiO_2 films deposited by evaporation in the same system at normal incidence have a refractive index of $n = 2.25$. Therefore, assuming that the nanorod film contains a mixture of TiO_2 and air, we estimate that it is comprised of a 65:35 mixture of air:TiO_2, assuming a linear relation for a combination of two materials. The GLAD results in the formation of narrow TiO_2 rods with a height of ~85 nm and a lean angle of ~35° towards the deposition flux. The rod diameter and spacing between rods are difficult to estimate due to the random structure of the film and the observed degree of rod taper. Due to the orientation of the sensor grating structure with respect to the deposition source, the nanorod film is added to both the upper and lower horizontal surfaces of the PC, although little or no deposition is observed on the sidewalls.

Fig. 3 shows the resonant reflection spectrum of both the uncoated sensor and the nanorod-coated sensor. The additional nanorod layer causes a positive shift of the measured PWV by 21.83 nm, but does not result in significant broadening or shortening of the resonant peak. This result is important because the deposited nanorod structure, with feature sizes far below the resonant wavelength of ~880 nm, does not cause scatter-

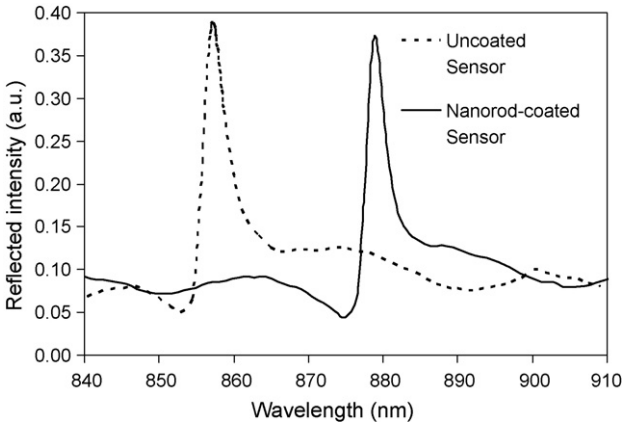

Fig. 3. Resonant reflection spectrum of uncoated and nanorod-coated sensors immersed in water. Note that the resonant peak width and peak height of the sensor are not diminished by the presence of the nanorod film.

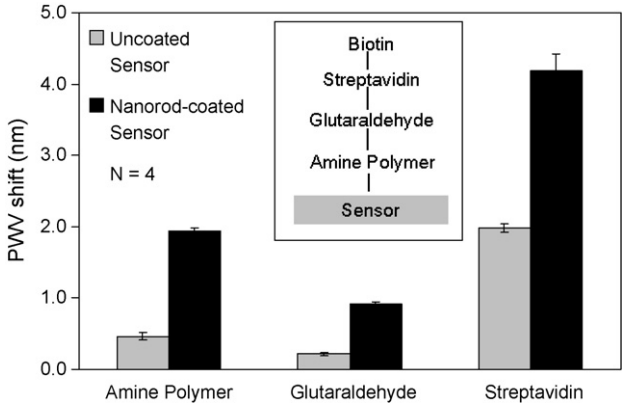

Fig. 4. PWV shifts of the amine polymer, glutaraldehyde and streptavidin steps for uncoated and nanorod-coated sensors.

ing or absorption that results in a measurable effect other than the addition of material with higher dielectric permittivity than water.

The PWV shifts measured as a result of the first three steps (Polymer, GA, SA) of the assay protocol are shown in Fig. 4, in which the measured PWV shift for each step is compared between uncoated and nanorod-coated sensors, with error bars indicating the standard deviation of four identical sensor wells measured independently for each condition. In each of these steps, the nanorod-coated sensors demonstrated higher sensitivity than the uncoated sensors. The enhancement effect was most pronounced for attachment of the amine polymer film (4.18× enhancement) and functionalization of the amine polymer by GA (4.30× enhancement). Covalent attachment of the large SA molecule demonstrated an enhancement of 2.11× due to the nanorod film, indicating that the surface structure was penetrated more easily by the polymer and glutaraldehyde molecules than by a large protein with a globular structure.

A measurement of the PWV shift as a function of time for the biotin exposure after subtraction of the nonspecific binding signal from the reference sensor wells is shown in Fig. 5, with error bars indicating the standard deviation of four identical sensor wells measured simultaneously for each type of sensor. Assuming a 1:4 binding stoichiometry between immobilized SA and

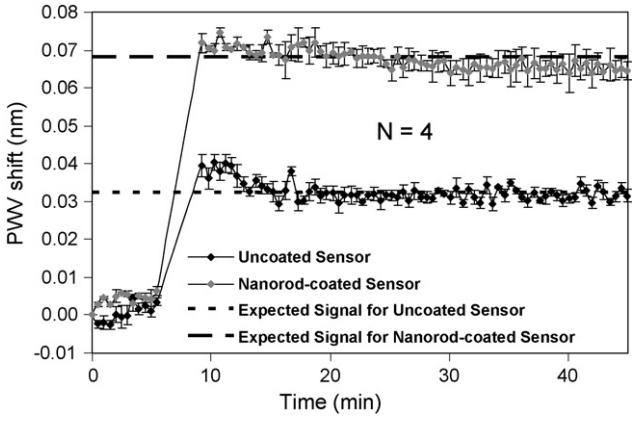

Fig. 5. Kinetics of the biotin binding step for both uncoated and nanorod-coated sensors.

detected biotin molecules, a "theoretically possible" PWV shift for biotin binding is indicated on Fig. 5, which is calculated using Eq. (1). Fig. 5 indicates that the measured biotin signal is 95% of the theoretically possible biotin PWV shift for the uncoated sensor and 94% for the nanorod-coated sensor. The biotin signal enhancement (2.07×) is comparable to the 2.11× signal enhancement obtained during SA attachment.

4. Discussion

In order to make a rough estimate of the expected additional surface area available due to the nanorod film, a simplified physical model was constructed based on the ellipsometer measurements of TiO_2 density. If we assume that the nanorod film consists of rods with the same diameter, arranged in a square lattice with equal spacing between adjacent rods, a film with a 65:35 air:TiO_2 ratio is obtained with a rod diameter of ∼30 nm and a gap of ∼15 nm between adjacent rods. We expect that a gap of ∼15 nm will allow permeation by a large variety of protein molecules, although this dimension may leave little additional space for "thick" surface functionalization film chemistry or for sandwich-type assays that stack multiple large molecules in sequence. Using this simple model, we estimate that rods with 85 nm height will result in a surface area enhancement of ∼4× compared to a flat surface.

The data in Fig. 4 indicates that the surface area increase may in fact be as high as 4×, when compared to a flat surface, as measured by the PWV shift due to polymer adsorption. It is interesting to note that the PWV shift measured due to GA functionalization of the polymer layer results in greater enhancement (4.30×) than the adsorbed polymer (4.18×), an effect that is observed on a consistent basis. Two causes are possible for this effect: (1) the polymer within the nanorod film adsorbs more GA molecules due to greater availability of functional amine groups on the nanorod structure compared to a flat surface, or (2) the GA has more opportunity to form cross-links in the polymer network, thus increasing its density, and thereby resulting in a higher observed PWV shift for the same mass of incorporated material. Future experiments will focus on separating these two mechanisms. The reduction of enhancement for covalent attachment of SA to the nanorod-coated sensor indicates that large globular molecules are not able to fully take advantage of all the available surface area. Although, the porous structure of the nanorod film may allow ∼2.11× higher density of immobilized SA, the structure did not appear to degrade the functionality of the immobilized protein, as measured by the availability of biotin binding sites. In addition, the kinetic rate of biotin attachment to SA within the nanorod film was measured to be nearly identical to that of a "flat" film, indicating that the small molecule analyte could easily diffuse to available binding sites.

Due to the simplicity of the deposition process and its potential for uniformity over large areas, we expect that nanorod films deposited by GLAD could be used to enhance the binding surface area for many types of chemical and biological sensors. The approach does not implicitly increase the sensitivity of a sensor, but rather, provides the capacity for the sensor to bind a greater mass of adsorbed material. This hypothesis is supported

by comparing the measured PWV shift obtained by exposing the uncoated sensors and nanorod-coated sensors to a "bulk" refractive index change from water ($n = 1.333$) to isopropyl alcohol ($n = 1.378$). Both uncoated and nanorod-coated sensors undergo a PWV shift = 7.1 nm, indicating that their inherent sensitivities are equal when no surface-adsorption mechanisms are involved in detection. Instead, this approach provides a small surface perturbation that results in capacity for adsorption of greater mass than a corresponding flat surface. As this work shows, the density of the surface must be engineered to enable molecules of a desired size to easily penetrate the film in order to obtain maximum benefit. In future work, we plan to further modify the GLAD process to produce more "open" film structures with greater nanorod height for applications in protein–protein interaction assays, and protein-small molecule screening.

5. Conclusion

In this work, we have demonstrated the sensitivity improvement of a PC biosensor through incorporation of a high surface area nanorod layer. Up to 4 times enhancement in sensitivity has been shown and the enhancement depends on the size and shape of the molecule that is deposited onto the sensor surface.

Acknowledgments

This work was supported by the National Science Foundation under Grant No. 0427657. Any opinions, findings, and conclusions or recommendations expressed in this material are those of the author(s) and do not necessarily reflect the views of the National Science Foundation. The authors gratefully acknowledge SRU Biosystems for providing financial support for this work. The authors also extend their gratitude to the support staff of the Micro and Nanotechnology Laboratory at the University of Illinois at Urbana-Champaign.

References

[1] B.T. Cunningham, P. Li, S. Schulz, B. Lin, C. Baird, J. Gerstenmaier, C. Genick, F. Wang, E. Fine, L. Laing, Label-free assays on the BIND system, Journal of Biomolecular Screening 9 (2004) 481–490.
[2] B.T. Cunningham, L. Laing, Microplate-based, label-free detection of biomolecular interactions: applications in proteomics, Expert Review of Proteomics 3 (2006) 271–281.
[3] B. Cunningham, B. Lin, J. Qiu, P. Li, J. Pepper, B. Hugh, A plastic colorimetric resonant optical biosensor for multiparallel detection of label-free biochemical interactions, Sensors and Actuators B-Chemical 85 (2002) 219–226.
[4] B. Cunningham, P. Li, B. Lin, J. Pepper, Colorimetric resonant reflection as a direct biochemical assay technique, Sensors and Actuators B-Chemical 81 (2002) 316–328.
[5] I.D. Block, L.L. Chan, B.T. Cunningham, Photonic crystal optical biosensor incorporating structured low-index porous dielectric, Sensors and Actuators B-Chemical 120 (2006) 187–193.
[6] N. Ganesh, I.D. Block, B.T. Cunningham, Near ultraviolet-wavelength photonic-crystal biosensor with enhanced surface-to-bulk sensitivity ratio, Applied Physics Letters 89 (2006), 023901.
[7] C.Y. Kuo, S.Y. Lu, S. Chen, M. Bernards, S. Jiang, Stop band shift based chemical sensing with three-dimensional opal and inverse opal structures, Sensors and Actuators B-Chemical 124 (2007) 452–458.
[8] Y.J. Lee, S.A. Pruzinsky, P.V. Braun, Glucose-sensitive inverse opal hydrogels: analysis of optical diffraction response, Langmuir 20 (2004) 3096–3106.
[9] E. Chow, A. Grot, L.W. Mirkarimi, M. Sigalas, G. Girolami, Ultracompact biochemical sensor built with two-dimensional photonic crystal microcavity, Optics Letters 29 (2004) 1093–1095.
[10] M. Lee, P.M. Fauchet, Two-dimensional silicon photonic crystal based biosensing platform for protein detection, Optics Express 15 (2007) 4530–4535.
[11] N. Skivesen, A. Tetu, M. Kristensen, J. Kjems, L.H. Frandsen, P.I. Borel, Photonic-crystal waveguide biosensor, Optics Express 15 (2007) 3169–3176.
[12] H. Kurt, D.S. Citrin, Photonic crystals for biochemical sensing in the terahertz region, Applied Physics Letters 87 (2005), 041108.
[13] S. Lofas, B. Johnsson, A novel hydrogel matrix on gold surfaces in surface-plasmon resonance sensors for fast and efficient covalent immobilization of ligands, Journal of the Chemical Society-Chemical Communications (21) (1990) 1526–1528.
[14] S. Lofas, Dextran modified self-assembled monolayer surfaces for use in biointeraction analysis with surface-plasmon resonance, Pure and Applied Chemistry 67 (1995) 829–834.
[15] V.S.Y. Lin, K. Motesharei, K.P.S. Dancil, M.J. Sailor, M.R. Ghadiri, A porous silicon-based optical interferometric biosensor, Science 278 (1997) 840–843.
[16] I. Rendina, I. Rea, L. Rotiroti, L. De Stefano, Porous silicon-based optical biosensors and biochips, Physica E-Low-Dimensional Systems & Nanostructures 38 (2007) 188–192.
[17] L. De Stefano, M. Rossi, M. Staiano, G. Mamone, A. Parracino, L. Rotiroti, I. Rendina, M. Rossi, S. D'Auria, Glutamine-binding protein from Escherichia coli specifically binds a wheat gliadin peptide allowing the design of a new porous silicon-based optical biosensor, Journal of Proteome Research 5 (2006) 1241–1245.
[18] S. Chan, Y. Li, L.J. Rothberg, B.L. Miller, P.M. Fauchet, Nanoscale silicon microcavities for biosensing, Materials Science & Engineering C-Biomimetic and Supramolecular Systems 15 (2001) 277–282.
[19] J.E. Lugo, M. Ocampo, A.G. Kirk, D.V. Plant, P.M. Fauchet, Electrochemical sensing of DNA with porous silicon layers, Journal of New Materials for Electrochemical Systems 10 (2007) 113–116.
[20] S. Mathur, V. Sivakov, H. Shen, S. Barth, C. Cavelius, A. Nilsson, P. Kuhn, Nanostructured films of iron, tin and titanium oxides by chemical vapor deposition, Thin Solid Films 502 (2006) 88–93.
[21] K.D. Benkstein, C.J. Martinez, G.F. Li, D.C. Meier, C.B. Montgomery, S. Semancik, Integration of nanostructured materials with MEMS microhotplate platforms to enhance chemical sensor performance, Journal of Nanoparticle Research 8 (2006) 809–822.
[22] C.J. Martinez, B. Hockey, C.B. Montgomery, S. Semancik, Porous tin oxide nanostructured microspheres for sensor applications, Langmuir 21 (2005) 7937–7944.
[23] M.R. Mohammadi, D.J. Fray, M.C. Cordero-Cabrera, Sensor performance of nanostructured TiO_2 thin films derived from particulate sol–gel route and polymeric fugitive agents, Sensors and Actuators B-Chemical 124 (2007) 74–83.
[24] N. Levit, D. Pestov, G. Tepper, High surface area polymer coatings for SAW-based chemical sensor applications, Sensors and Actuators B-Chemical 82 (2002) 241–249.
[25] K. Robbie, L.J. Friedrich, S.K. Dew, T. Smy, M.J. Brett, Fabrication of thin-films with highly porous microstructures, Journal of Vacuum Science & Technology a-Vacuum Surfaces and Films 13 (1995) 1032–1035.
[26] J.Q. Xi, J.K. Kim, E.F. Schubert, D.X. Ye, T.M. Lu, S.Y. Lin, J.S. Juneja, Very low-refractive-index optical thin films consisting of an array of SiO_2 nanorods, Optics Letters 31 (2006) 601–603.
[27] K. Robbie, A.J.P. Hnatiw, M.J. Brett, R.I. MacDonald, J.N. McMullin, Inhomogeneous thin film optical filters fabricated using glancing angle deposition, Electronics Letters 33 (1997) 1213–1214.
[28] K. Robbie, D.J. Broer, M.J. Brett, Chiral nematic order in liquid crystals imposed by an engineered inorganic nanostructure, Nature 399 (1999) 764–766.

[29] S.B. Chaney, S. Shanmukh, Y.-P. Zhao, R.A. Dluhy, Aligned silver nanorod arrays produce high sensitivity SERS substrates, Applied Physics Letters 87 (2005) 031908.
[30] Y.P. Zhao, S.H. Li, S.B. Chaney, S. Shanmukh, J.G. Fan, R.A. Dluhy, W. Kisaalita, Designing nanostructures for sensor applications, Journal of Electronic Materials 35 (2006) 846–851.
[31] S.S. Wang, R. Magnusson, J.S. Bagby, M.G. Moharam, Guided-mode resonances in planar dielectric-layer diffraction gratings, Journal of the Optical Society of America a-Optics Image Science and Vision 7 (1990) 1470–1474.
[32] S.S. Wang, R. Magnusson, Theory and applications of guided-mode resonance filters, Applied Optics 32 (1993) 2606–2613.
[33] C.S. Neish, I.L. Martin, R.M. Henderson, J.M. Edwardson, Direct visualization of ligand-protein interactions using atomic force microscopy, British Journal of Pharmacology 135 (2002) 1943–1950.
[34] P.C. Weber, M.J. Cox, F.R. Salemme, D.H. Ohlendorf, Crystallographic data for streptomyces-avidinii streptavidin, Journal of Biological Chemistry 262 (1987) 12728–12729.
[35] P.C. Weber, D.H. Ohlendorf, J.J. Wendoloski, F.R. Salemme, Structural origins of high-affinity biotin binding to streptavidin, Science 243 (1989) 85–88.

Biographies

Wei Zhang received a BS in applied physics from the University of Science and Technology of China in 2002. He is currently working towards the PhD degree on thin film deposition, fabrication and characterization of high sensitivity photonic crystal biosensors in the Department of Materials Science and Engineering at the University of Illinois at Urbana-Champaign.

Nikhil Ganesh received a BE in polymer sciences and chemical technology from the Delhi College of Engineering, New Delhi, India in 2004. He is currently a PhD candidate in the Department of Materials Science and Engineering at the University of Illinois at Urbana-Champaign. His research interests include nanophotonics and biosensors.

Ian D. Block received a BS in electrical & computer engineering from Cornell University in 2004, and a MS in electrical engineering from the University of Illinois at Urbana-Champaign in 2005. He is currently working towards a PhD under the direction of Dr. Brian Cunningham at the University of Illinois. The focus of his research is the design and characterization of enhanced sensitivity photonic crystal biosensors.

Brian T. Cunningham is an associate professor of electrical and computer engineering at the University of Illinois at Urbana-Champaign, where he is the director of the nanosensors group. His group focuses on the development of photonic crystal-based transducers, plastic-based fabrication methods, and novel instrumentation approaches for label-free biodetection. Prof. Cunningham is a founder and the Chief Technical Officer of SRU Biosystems (Woburn, MA), a life science tools company that provides high sensitivity plastic-based optical biosensors, instrumentation, and software to the pharmaceutical, academic research, genomics, and proteomics communities. Prior to founding SRU Biosystems in June, 2000, Dr. Cunningham was the manager of Biomedical Technology at Draper Laboratory (Cambridge, MA), where he directed R&D projects aimed at utilizing defense-related technical capabilities for medical applications. In addition, Dr. Cunningham served as Group Leader for MEMS Sensors at Draper Laboratory, where he directed a group performing applied research on microfabricated inertial sensors, acoustic sensors, optical switches, microfluidics, tissue engineering, and biosensors. Concurrently, he was an associate director of the Center for Innovative Minimally Invasive Therapy (CIMIT), a Boston-area medical technology consortium, where he led the Advanced Technology Team on Microsensors. Before working at Draper Laboratory, Dr. Cunningham spent 5 years at the Raytheon Electronic Systems Division developing advanced infrared imaging array technology for defense and commercial applications. Dr. Cunningham earned his BS, MS, and PhD degrees in electrical and computer engineering at the University of Illinois. His thesis research was in the field of optoelectronics and compound semiconductor material science, where he contributed to the development of crystal growth techniques that are now widely used for manufacturing solid-state lasers, and high frequency amplifiers for wireless communication.